Proline-Directed Phosphorylation of the Dopamine Transporter N-Terminal Domain

ARTICLE *in* BIOCHEMISTRY · FEBRUARY 2009

Impact Factor: 3.02 · DOI: 10.1021/bi801696n · Source: PubMed

4 AUTHORS, INCLUDING:

Amy E Moritz
U.S. Department of Health and Human Services
7 PUBLICATIONS **68** CITATIONS
SEE PROFILE

James D Foster
University of North Dakota School of Medicin…
41 PUBLICATIONS **1,146** CITATIONS
SEE PROFILE

Roxanne A Vaughan
University of North Dakota
78 PUBLICATIONS **3,088** CITATIONS
SEE PROFILE

Published in final edited form as:
Biochemistry. 2009 February 10; 48(5): 1067–1076. doi:10.1021/bi801696n.

Proline-directed phosphorylation of the dopamine transporter N-terminal domain

Balachandra K. Gorentla, **Amy E. Moritz**, **James D. Foster**, and **Roxanne A. Vaughan***
Department of Biochemistry and Molecular Biology, University of North Dakota School of Medicine and Health Sciences, Grand Forks, ND 58201

Abstract

Phosphorylation of the dopamine transporter (DAT) on N-terminal serines and unidentified threonines occurs concomitantly with PKC- and substrate-induced alterations in transporter activity, subcellular distribution, and dopamine efflux, but the residues phosphorylated and identities of protein kinases and phosphatases involved are not known. As one approach to investigating these issues we recombinantly expressed the N-terminal tail of rat DAT (NDAT) and examined its phosphorylation and dephosphorylation properties *in vitro*. We found that NDAT could be phosphorylated to significant levels by PKCα, PKA, PKG, and CaMKII, which catalyzed serine phosphorylation, and ERK1, JNK, and p38, which catalyzed threonine phosphorylation. We identified Thr53, present in a membrane proximal proline-directed kinase motif as the NDAT site phosphorylated *in vitro* by ERK1, JNK and p38, and confirmed by peptide mapping and mutagenesis that Thr53 is phosphorylated *in vivo*. Dephosphorylation studies showed that protein phosphatase 1 catalyzed near-complete *in vitro* dephosphorylation of PKCα-phosphorylated NDAT, similar to its *in vivo* and *in vitro* effects on native DAT. These findings demonstrate the ability of multiple enzymes to directly recognize the DAT N-terminal domain and for kinases to act at multiple distinct sites. The strong correspondence between NDAT and rDAT phosphorylation characteristics suggests the potential for the enzymes that are active on NDAT *in vitro* to act on DAT *in vivo* and indicates the usefulness of NDAT for guiding future DAT phosphorylation analyses.

The dopamine transporter (DAT) is a plasma membrane phosphoprotein expressed in dopaminergic neurons that clears synaptic dopamine (DA) by Na^+-Cl^- dependent reuptake. This activity controls the availability of extracellular DA for binding to receptors and thus regulates the dynamics of dopaminergic neurotransmission (1). Processes controlled by DA include motor activity, emotion, and reward, and agents such as cocaine that inhibit DAT cause elevations in DA levels that lead to motor stimulation and addiction (2). DA levels are also increased by amphetamine (AMPH) and methamphetamine (METH), which are carried by DAT and induce DA efflux by the process of reverse transport (3,4). It is thought that dopaminergic disorders such as depression, schizophrenia, ADHD and Parkinson's disease may be linked to dysregulation of DAT activity and resulting imbalances in DA clearance (5-9).

Various properties of DAT are acutely regulated by protein kinases, protein phosphatases, and substrate pretreatments (10-12), indicating the ability of DAT to rapidly respond to physiological demands. Regulation of DA transport occurs in response to modulation of protein kinase C (PKC), extracellular-signal regulated protein kinase (ERK), protein kinase B (Akt), and protein phosphatases 1 and 2A (PP1/2A) (13-16), and PKC activity is required for substrate induced transport down-regulation (17-19). Kinase- and substrate-induced DA transport down-

*Roxanne A. Vaughan, Department of Biochemistry and Molecular Biology, University of North Dakota School of Medicine and Health Sciences, Grand Forks, ND 58201. Phone: 701−777−3419. Fax: 701−777−2382. Email: rvaughan@medicine.nodak.edu..

regulation are associated with alterations in DAT trafficking and surface levels (16,20-24) while PKC-induced transport regulation also occurs in part by a trafficking-independent process that is sensitive to cholesterol depletion (25). Basal and AMPH-stimulated DA efflux involve actions of PKC and CaMKII (4,15,26), and activation of PKC stimulates DAT phosphorylation, ubiquitylation and degradation (13,27,28). Thus it is clear that several functions of DAT are regulated by multiple phosphorylation pathways. The precise mechanisms by which most of these effects occur remain unknown, although DAT N-terminal phosphorylation has been reported to be required for AMPH-induced efflux and AMPH/METH-induced increases in intracellular Ca^{++} (29) but not for PKC or AMPH-induced DAT endocytosis and down-regulation (18,30).

In both rat striatal tissue and heterologous expression systems, DAT displays a tonic level of phosphorylation that is increased by PKC activators such as phorbol 12-myristate 13-acetate (PMA) and phosphatase inhibitors such as okadaic acid (OA) (13,18,30,31), implicating the activities of PKC and PP1/2A in DAT phosphate turnover. Reduced DAT phosphorylation has been found after pharmacological inhibition of ERK (32), suggesting a role for this kinase in maintenance of DAT phosphorylation. DAT phosphorylation is also stimulated by *in vivo* and *in vitro* AMPH and METH treatments via a PKC-dependent process (18), and PMA-induced phosphorylation is inhibited by *in vitro* application of the DA uptake blocker GBR 12909 (19) and at low PMA concentrations by cocaine (33), indicating a role for psychoactive drugs in regulation of transporter phosphorylation and accompanying processes. In addition, serine mutagenesis studies have suggested the phosphorylation of DAT by CaMKII as a mechanism underlying AMPH-induced DA efflux (15).

PKC- and OA-stimulated metabolic phosphorylation of rat striatal DAT has been mapped to a cluster of six closely spaced serines at the distal end of the N-terminal tail (Fig. 1A) (34), and mutagenesis of heterologously expressed rat (r) and human (h) DAT has confirmed utilization of sites in this domain (18,30). The precise residues within this domain that are phosphorylated remain unknown, although mutation and deletion studies indicate the use of multiple sites (32,35). This region contains consensus motifs for PKC, cAMP-dependent protein kinase (PKA), and CaMKII, while a second cluster of serines and threonines more proximal to the membrane contains consensus motifs for PKC, PKA, and proline-directed kinases (Fig. 1A). The DAT C-terminal tail also contains canonical PKC, PKA, and proline-directed kinase motifs (Fig. 1B). Although Ser and Thr residues in the C-terminal domain have been suggested as potential phosphorylation sites (36), little evidence currently supports this. Thus the N- and C-termini contain multiple potential phosphorylation sites for many of the kinases that affect DAT phosphorylation and/or regulation, but it is not known if these enzymes directly phosphorylate DAT, and if so, at which sites. This information is necessary for understanding the mechanisms by which phosphorylation regulates DAT and determining if kinase-mediated regulatory processes occur through phosphorylation of DAT or through effects on interacting proteins. As one approach to investigating these issues, we recombinantly expressed the N- and C-terminal domains of rDAT (NDAT and CDAT) and used the peptides for *in vitro* phosphorylation and dephosphorylation studies. Our results show that NDAT is an excellent substrate for multiple protein kinases and phosphatases, and that different kinases act on the peptide at different sites. This demonstrates the ability of these enzymes to directly interact with DAT and indicates the potential for these enzymes to act on DAT *in vivo*. Robust NDAT *in vitro* threonine phosphorylation catalyzed by proline-directed kinases was found Thr53, and mutagenesis of Thr53 in the full length protein caused loss of metabolically incorporated phosphothreonine, identifying this residue as the origin of phosphothreonine in DAT and providing the first evidence for proline-directed phosphorylation of DAT.

METHODS

Cloning of DAT N- and C-terminal domains

The rDAT N- and C-terminal tail sequences shown in Fig. 1 (NDAT and CDAT) were inserted into Intein recombinant expression vectors that fuse the protein of interest to Chitin Binding Domain (CBD, molecular mass ~55 kDa) via a sulfhydryl cleavable bond. The wild type (WT) rDAT cDNA in a pcDNA 3.0 vector (18) was used for cloning. The open reading frame encoding amino acids 1−65 was PCR amplified and subcloned into the pTYB2 expression vector (New England Biolabs) to generate NDAT linked via its C-terminus to CBD. The open reading frame encoding amino acids 579−619 was amplified and subcloned into the pTYB1 expression vector to generate CDAT linked via its N-terminus to CBD. NDAT threonine (T) to alanine (A) substitutions were generated in the pTYB2-NDAT construct using the Stratagene QuikChange® kit. Accuracy of all constructs was verified by sequencing (Alpha Biolabs, CA).

Expression and purification of NDAT and CDAT

E. coli T7 express cells (New England Biolabs) were transformed with NDAT-pTYB2 or CDAT-pTYB1 and colonies selected from LB agar plates containing 50 μg/ml of carbenicillin. Transformed colonies were inoculated into LB medium containing 50 μg/ml carbenicillin and grown at 37 °C to an OD_{600} of 0.8. Fusion protein expression was induced with 0.5 mM isopropyl β-D-1-thiogalactopyranoside (IPTG) for 16 h at 16 °C. Bacteria were pelleted by centrifugation at 5000 *g* for 10 min at 4 °C, resuspended with ice cold lysis buffer (50 mM Tris, pH 7.5, 150 mM NaCl, 0.05% Triton X-100 and one Roche Complete Mini protease inhibitor tablet), and lysed by passage through a French pressure cell. The resulting crude extract was centrifuged at 20,000 *g* for 30 min to sediment particulate elements, and analysis of pellets and supernatants indicated >95% recovery of NDAT-CBD and CDAT-CBD in the soluble fraction.

NDAT-CBD and CDAT-CBD fusion proteins were isolated from crude *E. coli* lysate by chromatography on chitin-Sepharose. Lysates were incubated with chitin-Sepharose resin for 18 h at 4 °C, the unbound fraction was collected, and the resin was washed with 10 bed volumes of column buffer (50 mM Tris, pH 7.5, 500 mM NaCl, 1 mM EDTA). NDAT and CDAT were released from CBD by two sequential incubations of the resin with 3 bed volumes of column buffer containing 50 mM dithiothreitol (DTT) for 40 h at 4 °C. The eluted fragments were dialyzed extensively against 20 mM MOPS pH 7.4, and concentrated to 1−10 mg/ml by spin filtration. Protein levels were determined using the BioRad protein assay kit and peptides were estimated to be >95% pure by Commassie staining.

In vitro phosphorylation assays

1.5 μg of NDAT or CDAT were suspended in 20 mM MOPS pH 7.4 containing 5 mM $MgCl_2$, 300 μM $CaCl_2$, 40 μM ATP, 12 μCi [γ-^{32}P]ATP and additional components as indicated below in a final volume of 75 μl. Reactions were initiated by adding purified recombinant kinases and were performed at 30 °C for 30 min and terminated by addition of 100 mM EDTA. Additional specific reagents included were 40 μg/ml dioleoylphosphatidylserine and 1.6 μg/ml diacylglycerol for all PKC isoforms; 2.4 μM calmodulin for CaMKII; and 10 μM 8-Br cGMP for PKG. Enzyme amounts used were calculated to provide equal specific activities (1 nmol phosphate transfer to model substrate/min) based on information provided by vendors, and all kinases were highly active against histones or myelin basic protein (not shown). Following *in vitro* phosphorylation, NDAT and CDAT samples were immunoprecipitated with polyclonal antibody (Ab) 16 generated against rDAT N-terminal amino acids 42−59 (Fig. 1A) or DAT C-terminal antibody from Chemicon. Precipitated samples were electrophoresed on 10−20% SDS polyacrylamide gels using low and high range Rainbow molecular mass markers as standards, and gels were dried and

subjected to autoradiography at −70 °C using Kodak Biomax film for 2−48 h or were transferred to PVDF for immunoblotting. For immunoblotting, PVDF membranes were probed with DAT N-terminal monoclonal Ab16 (mAb16) and developed as described (37). Autoradiographs and immunoblots were scanned and band densities quantified with BioRad Molecular Analyst software (19,31). For quantification of relative *in vitro* phosphorylation levels, the densitometric values of NDAT phosphorylated by PKCα or ERK1, as indicated, were normalized to 100% and values for other kinases expressed as a fraction thereof. All experiments were performed two or more times with similar results.

In vitro dephosphorylation assay

NDATs phosphorylated *in vitro* by PKCα or ERK1 were immunoprecipitated with Ab16 and *in vitro* dephosphorylation was assessed in triplicate using immune complexes bound to protein A Sepharose beads. The reaction mixtures consisted of 20 mM MOPS pH 7.4, 200 μM $MnCl_2$, 5 mM DTT, 100 μM EDTA, 0.2% BSA and purified PP1, PP2A, or PP2B, in a final volume of 500 μl. PP2B reactions also contained 1 μM calmodulin and 1 mM $CaCl_2$. Enzyme amounts used were calculated to provide equal specific activities (1 nmol phosphate hydrolyzed from model substrate/min) based on information provided by vendors, and all were active against synthetic substrates as described (38). Reactions were performed for 2 h at 22 °C followed by elution of proteins from beads with sample buffer and analysis by SDS-PAGE/autoradiography or immunoblotting. Parallel reactions were performed with immunoprecipitated metabolically phosphorylated rat striatal DAT to compare dephosphorylation patterns of NDAT and rDAT. Autoradiographs were scanned and ^{32}P labeling intensities of untreated samples were defined as 100% with treatment values expressed as a fraction therof. Normalized phosphorylation values from multiple experiments were averaged and analyzed statistically by analysis of variance (ANOVA) using Prism 3 software.

Asp-N proteolysis of rDAT

Membranes were prepared from rat striatal slices metabolically labeled with $^{32}PO_4$ and treated with OA and oleoyl acetyl glycerol (OAG) to stimulate DAT phosphorylation, followed by *in situ* proteolysis with endoproteinase Asp-N as described previously (34). Membranes were solubilized and DAT and DAT fragments were subjected to immunoprecipitation with Ab16 followed by electrophoresis, autoradiography, and phosphoamino acid analysis.

T53A mutagenesis

The T53A mutation was made in the rDAT pcDNA 3.1 template using the Stratagene quick change kit followed by sequencing of the entire DAT region to ensure accuracy. $LLCPK_1$ cells were stably transfected with the vector using FuGENE transfection reagent and maintained under selection with 600 μg/ml G418. Total and surface DAT expression and DA uptake kinetic parameters of the T53A DAT were not significantly different from the WT protein (not shown).

Phosphoamino acid analysis

NDAT, rDAT, and Asp-N fragments were subjected to phosphoamino acid analysis by two-dimensional thin layer chromatography (2D TLC) (39). ^{32}P-labeled samples prepared as described above were electrophoresed on SDS-PAGE, detected by autoradiography and excised. Protein was electroeluted, dialyzed against distilled water, acetone precipitated, and hydrolyzed with 5.7 M HCl for 2 h at 110 °C. The resulting samples were suspended in pH 1.9 buffer (acetic acid 7.8%, formic acid 2.5%) and mixed with10 μg unlabeled phosphoserine (pSer), phosphothreonine (pThr), and phosphotyrosine (pTyr) standards. Samples were spotted onto cellulose thin layer plates and electrophoresed using a Hunter thin layer electrophoresis unit at 1.5 kV for 35 min at pH 1.9 in the first dimension and at 1.3 kV for 20 min at pH 3.5

(pyridine 0.5%, acetic acid 5%) in the second dimension. Standards were visualized with ninhydrin and the plates were subjected to autoradiography for 1−3 weeks.

Materials

IMPACT-CN® bacterial cloning and expression kit, restriction enzymes, and modifying enzymes were from New England Bio labs (Ipswich MA, USA); [γ^{32}P]ATP (specific activity 7000 Ci/ml) and carrier-free $^{32}PO_4$ were from ICN; low and high range Rainbow molecular mass standards were from GE Health care; protein kinases, protein phosphatases, OA, OAG and endoproteinase AspN were from Calbiochem (San Diego, CA, USA); QuikChange® mutagenesis kit was from Stratagene (La Jolla, CA, USA); Complete Mini protease inhibitor tablets were from Roche Applied Bioscience (Indianapolis, IN, USA); isopropyl β-D-1-thiogalactopyranoside (IPTG) and all other fine chemicals were from Sigma (St. Louis, MO, USA). All kinases used were expressed recombinantly and were human isoforms except for CaMKII and PKGIα which were rat and bovine isoforms, respectively. ERK1, ERK2, and Akt were phosphorylation activated. PP1α and PP2B were recombinant rabbit and human isoforms, respectively. PP2A was from bovine kidney. All enzymes were highly purified (> 90−95%) as indicated by vendor's information.

RESULTS

Generation of recombinant NDAT

IPTG induction of *E coli* cells transformed with the NDAT-pTBY2 vector (Fig. 2A) caused robust production of NDAT-CBD fusion protein which is visible at ~65 kDa in lane 2 (*arrow a*) but not seen in non induced cells (lane 1). The fusion protein was isolated from crude lysates by chromatography on chitin-Sepharose resin. NDAT-CBD bound to the resin and was not present at significant levels in the column flow-through (lane 3) or final wash fraction (lane 4). NDAT was released from CBD by incubation of resin with DTT and is visible as the major band at the expected mass of ~7 kDa (lanes 5 and 6). The fragment was strongly reactive with N-terminal Ab16 in immunoblotting (lanes 7 and 8) and immunoprecipitation assays (Fig. 2B, lower panel). Minor amounts of higher M_r NDAT aggregates were also visible in Coommassie stained and immunoblotted samples. Similar to the pattern obtained with rDAT (Fig. 2B, upper panel), NDAT precipitation with Ab16 (Fig. 2B, lane 2) was blocked by antibody preabsorption with immunizing peptide (lane 3), and was not obtained with pre-immune antiserum (lane 4), verifying the identity of the recombinant peptide. These procedures produce a final yield of 2−5 mg of NDAT per liter of *E. coli* culture with an estimated purity of >95%.

Multiple kinases phosphorylate NDAT *in vitro*

We then tested the ability of NDAT to serve as an *in vitro* substrate for various purified serine/threonine kinases. Because of the substantial evidence demonstrating PMA stimulation of DAT metabolic phosphorylation, our initial studies focused on PKC (Fig. 3). Lane 1 (upper panel) shows an autoradiograph of NDAT ^{32}P labeling catalyzed by PKCα. Labeling was blocked by chelation of Mg^{2+} with EDTA to prevent phosphoryl transfer (lane 2), and reactions in which either NDAT or PKCα were absent showed no ^{32}P labeled product (lanes 3 and 4). Western blotting demonstrated the presence of NDAT in all pertinent reactions (lower panel). These controls substantiate the identities of the phosphorylated product as NDAT and the kinase as PKCα, and validate the assay as demonstrating NDAT *in vitro* phosphorylation.

We then extended these studies to other kinases (Fig. 4), using equal enzyme activities for each reaction. Figures 4A and 4C show representative results from separate experiments in which the kinases indicated in each panel were tested in parallel. Upper rows of each panel show autoradiographs of ^{32}P incorporation and lower rows show immunoblots verifying equal NDAT loading. The results show that NDAT was capable of serving as an *in vitro* substrate

for PKCα, PKCβI, PKCβII, PKCγ, ERK1, ERK2, CaMKII, PKA catalytic subunit, cGMP dependent protein kinase (PKG), casein kinase II (CKII), p38, c-Jun-N-terminal kinase (JNK), cyclin dependent kinase 5 (Cdk5), and Akt. Of the kinases we tested only GSK3β failed to catalyze detectable NDAT phosphorylation. Marked differences in ^{32}P labeling were observed (Fig. 4B and 4D), with comparable levels obtained with PKCα, PKA, CaMKII, and CKII; considerably higher levels catalyzed by ERK1/2, JNK, p38, PKG, and Cdk5; and lower levels catalyzed by PKCβI, PKCβII, PKCγ, and Akt.

The highest level of NDAT phosphorylation in these experiments was consistently obtained with the proline-directed kinases ERK1/2, p38, and JNK, which catalyzed 5−8 times more ^{32}P incorporation than PKCα (Fig. 4B). Immunoblots of NDAT phosphorylated by ERK1/2, p38 and JNK showed a discrete upward electrophoretic mobility shift compared to NDAT that was unphosphorylated or phosphorylated by other kinases (Figs. 4, 5 and 7), with the fraction of NDAT present in the upper band ranging from 25−75% of the total sample. Alignment of autoradiographs with immunoblots of radiolabeled samples showed that all of the ^{32}P was associated with the upper band, suggesting that phosphorylation of NDAT by these kinases induced a conformational change that resulted in reduced electrophoretic mobility. Confirmation that the shift was induced by phosphorylation was obtained in studies described below.

Further characterization of NDAT phosphorylation by PKCα and ERK1 showed that at the NDAT concentrations used in these experiments, ^{32}P labeling was linear up to 2 h of incubation, with no significant increases in labeling observed with higher doses of enzyme (not shown), indicating that under these conditions NDAT phosphorylation progressed to near completion. At the concentrations of PKCα and ERK1 used in these studies, NDAT saturation analyses generated K_ms of 2.5 μM and 4 μM, respectively (not shown). These values are comparable to or lower than the K_ms of many kinases for peptide substrates [39, 40], indicating that NDAT is an excellent substrate for these enzymes. Because the NDAT electrophoretic mobility shift induced by ERK1 is caused by phosphorylation, the fraction of shift (25−75%) provides an estimated phosphorylation stoichiometry of 0.25−0.75 mol phosphate/mol protein for ERK1. A comparable stoichiometry estimate of ~0.2 mole phosphate/mole protein was obtained by scintillation counting of ^{32}P labeled NDAT. Comparison of samples phosphorylated in parallel by PKCα, CaMKII, PKA, and PKG then generates estimates of approximately 0.05−0.15 mol phosphate/mol protein for these enzymes. The significantly lower levels of NDAT phosphorylation catalyzed by PKCβI, PKCβII, PKCγ, and Akt are consistent with low affinity/low stoichiometry interactions that may be less likely to occur physiologically, and further studies with these enzymes were not performed.

In vitro dephosphorylation of NDAT

We then used NDAT phosphorylated by PKCα or ERK1 as a substrate for analysis of *in vitro* dephosphorylation by purified PP1, PP2A or PP2B, and monitored dephosphorylation of rDAT in parallel (Fig. 5). The phosphatases were used at equal specific activities and all were active against model substrates as previously described (38). Phosphorylation levels were monitored by SDS-PAGE/autoradiography (middle row) and western blotting confirmed the presence of equal amounts of NDAT or rDAT in all samples (upper row). Quantification of ^{32}P labeling relative to control samples is shown in histograms (lower row). For NDAT phosphorylated by PKCα the greatest level of dephosphorylation was catalyzed by PP1, which removed 88 ± 3% of the ^{32}P label, a lesser amount was catalyzed by PP2B which removed 35 ± 10% of the ^{32}P label, and no dephosphorylation was obtained with PP2A (Fig. 5B). A similar profile was obtained for rDAT metabolically phosphorylated under PKC stimulation conditions (Fig. 5A) suggesting the similarity of phosphatase action on NDAT and full-length

DAT. In contrast to these results, treatment of ERK1-phosphorylated NDAT with these phosphatases caused no removal of ^{32}P or alteration in electrophoretic mobility shift (Fig. 5C).

Phosphoamino acid analysis of NDAT

The N-terminal tail of DAT contains 8 serines and 4 threonines (Fig. 1A). To determine the type of amino acid phosphorylated in NDAT, we subjected PKCα and ERK1 phosphorylated NDAT to phosphoamino acid analysis (Fig. 6). The results show that phosphorylation of NDAT by PKCα occurred to detectable levels only on Ser while phosphorylation catalyzed by ERK1 occurred only on Thr, demonstrating the use of distinct sites by these kinases. Phosphorylation of NDAT by PKA, PKG and CaMKII also occurs exclusively on Ser (40).

Identification of ERK phosphorylation site

In an attempt to identify the sites of PKCα phosphorylation on NDAT we constructed individual S→A substitutions of the first five serines, and found that phosphorylation was reduced but not eliminated in some of the mutants, indicating that PKCα phosphorylates NDAT at multiple sites (40). This parallels mutagenesis findings consistent with occurrence of PMA-stimulated rDAT metabolic phosphorylation on multiple serines (35), and we are currently attempting to ascertain the precise pattern of NDAT phosphorylation by PKCα.

To investigate ERK phosphorylation sites we generated individual T→A substitutions of NDAT at positions 43, 46, 53, and 62 and subjected the mutants to *in vitro* phosphorylation with ERK1 (Fig. 7A). The T43A, T46A, and T62A NDATs displayed ^{32}P labeling that was not less than the WT levels (upper panel) and showed the upward electrophoretic mobility shift (lower panels), while T53A NDAT showed no ^{32}P labeling or upward shift. T53A NDAT treated with p38 or JNK also showed no ^{32}P incorporation or mobility shift (not shown). These results indicate that Thr53 is the sole phosphorylation site for ERK1, p38, and JNK, and verify that the mobility shift is caused by phosphorylation.

In rDAT Thr53 is located in a sequence (P-P-Q-T-P) that conforms to an optimal proline-directed kinase consensus motif (P-P-X-S/T-P, where P is proline and X is any amino acid) (41) that is consistent with its use *in vitro*. An analogous proline-directed phosphorylation motif (P-R-Q-S-P) is present in hDAT (Fig. 1A), indicating the conservation of the sequence. The C-terminal tail of rDAT contains a minimal proline-directed phosphorylation sequence (S/T-P) at residues Thr595-Pro596, a site that is not conserved in hDAT (Fig. 1B). To determine if the C-terminal site of rDAT also undergoes phosphorylation, we expressed and purified the CDAT recombinant protein extending from residues 579−619 (approximate mass 4 kDa) in a manner analogous to that of NDAT, and subjected the peptide to *in vitro* phosphorylation. Figure 7b shows that ERK1 does not phosphorylate CDAT under the conditions positive for NDAT, indicating the specificity of NDAT phosphorylation by ERK. CDAT is also a negligible substrate for PKCα, with a phosphorylation level of <10% of that of PKCα-phosphorylated NDAT.

In vivo threonine phosphorylation of DAT occurs on the N-terminal tail

To probe the potential similarities between NDAT and rDAT threonine phosphorylation, we directed our efforts to determining the site of metabolic threonine phosphorylation on rDAT. Phosphoamino acid analysis of ^{32}P-labeled rat striatal DAT has shown the presence of pSer and pThr at about a 10:1 ratio (34). However, the origin of pThr in DAT is unknown, as the major site of metabolic phosphorylation at the distal end of the N-terminus contains no Thr residues (Fig. 1A), and there are numerous Thr in the N- and C-termini and intracellular loops that could function as phosphorylation sites.

To determine the origin of pThr on native DAT we used peptide mapping with endoproteinase Asp-N in combination with phosphoamino acid analysis. Asp-N cleaves DAT at Asp175 at the extracellular end of transmembrane domain (TM) 3, generating a 19 kDa fragment that extends from the N-terminus through TMs 1−3 (34). This fragment contains only six threonines (Thr43, Thr46, Thr53, Thr62, Thr144, Thr172), and molecular modeling strongly suggests that only the four in the N-terminal tail are intracellularly oriented and thus capable of serving as phosphate acceptors, while the other two are embedded in membrane or oriented extracellularly (42). This strategy thus provides a method for analyzing phosphorylation of N-terminal Thr residues independently of sites elsewhere in the protein.

For this experiment, we metabolically labeled rat striatal slices with ^{32}P in the presence of OA and OAG to stimulate DAT phosphorylation, and subjected membranes prepared from the slices to *in situ* proteolysis with Asp-N. The samples were precipitated with Ab16 to isolate the ^{32}P-labeled full-length DATs and the N-terminal Asp-N fragment (Fig. 8A), and the bands were excised from the gel and subjected to phosphoamino acid analysis. Equal counts were loaded to permit comparison of pSer and pThr ratios, and samples precipitated with preimmune antiserum were processed in parallel to test for signal specificity.

Fig. 8B shows that both pSer and pThr are present in full length DAT and the Asp-N fragment. No radioactive pSer or pThr were obtained from samples precipitated with preimmune serum (not shown), verifying that the extracted phosphoamino acids originated from DAT. Because the only intracellular threonines in the Asp-N fragment are the four in the N-terminal tail, this result identifies one or more of these residues as a source of pThr in neuronal DAT. In addition, because all known serine phosphorylation on DAT originates from the N-terminal tail, the similar ratios of pSer and pThr in full-length DAT and the Asp-N fragment indicate that a significant fraction of the pThr in the intact protein originates from the N-terminus.

To determine if Thr53 represents the site of phosphothreonine incorporation on DAT we expressed the T53A rDAT mutant and performed phosphoamino acid analysis of ^{32}P metabolically labeled protein. In preliminary experiments we found that T53A rDAT displayed basal and PMA-stimulated phosphorylation that was not qualitatively different from the WT phosphorylation pattern (not shown). Fig. 9A shows the phosphorylation profile of the WT and T53A proteins and a sample from DAT-null cells that was labeled and processed in parallel to serve as a specificity control. The DAT regions of these gels were excised and the extracted proteins processed for phosphoamino acid analysis. Both pSer and pThr were obtained from the WT protein (Fig. 9B, *left*), while no detectable radioactivity was obtained from the parent cells (not shown) verifying that the observed pSer and pThr signals originated from DAT. The T53A protein yielded pSer as expected, as the N-terminal serine cluster was unaffected by the mutation, but importantly showed no pThr signal (Fig. 9B, *right*), strongly suggesting that Thr53 represents a major site of metabolic pThr incorporation on DAT. This result has been replicated in an independently executed experiment.

Several studies have shown that ERK inhibitors reduce DA uptake (14,16). To determine if phosphorylation of DAT at Thr53 is involved in this response, we treated cells expressing WT and T53A rDAT to vehicle or the ERK inhibitor PD98059 and assayed for DA transport activity. Compared to control treatments, transport activity after treatment of cells with 50 μM PD98059 for 30 min was reduced to 63 ± 2% in the WT cells and to 70 ± 3% in the T53A cells, indicating that down-regulation to this treatment is not dependent on the phosphorylation state of Thr53. Acute down-regulation of transport to 1 μM PMA was also not affected by the mutation (not shown).

DISCUSSION

In this study, we found that NDAT was an excellent substrate for *in vitro* phosphorylation by PKCα, CaMKII, PKA, PKG, ERK1/2, p38, and JNK, and for *in vitro* dephosphorylation by PP1 and PP2B, demonstrating the capability of these enzymes to directly act on the DAT N-terminal domain. Many of the *in vitro* phosphorylation characteristics we found were highly similar to what had been previously known for *in vivo* phosphorylation, including the presence of pSer and pThr on NDAT and the rDAT N-terminal tail, localization of PKC-mediated phosphorylation to multiple sites in the distal N-terminal serine cluster, the most robust dephosphorylation catalyzed by PP1, and negligible phosphorylation occurring on CDAT or rDAT C-terminus. These characteristics in conjunction with the good stoichiometry and kinetic values of the *in vitro* reactions support the potential for these enzymes to act on DAT *in vivo*. The *in vitro* findings also led us to examine additional conditions related to PKA, PKG, and proline-directed kinases that have now considerably expanded our understanding of DAT phosphorylation characteristics.

The kinases we tested that strongly phosphorylated NDAT on Ser were PKCα, PKA, PKG, and CaMKII. DAT metabolic phosphorylation has been well characterized to be stimulated by PMA, activation of PKC-linked receptors, and METH and AMPH via a PKC-dependent pathway (13,18,30,34). In all of these cases the site of phosphorylation has been localized to the distal N-terminal serine cluster, thus the phosphorylation of NDAT on Ser by PKCα strongly supports the potential for the *in vivo* phosphorylation stimulated under these conditions to be catalyzed directly by PKCα. With respect to other kinases, we have recently found that DAT phosphorylation is increased by activators of PKA and PKG (A. Moritz and R. Vaughan, unpublished results), which could potentially be consistent with the NDAT results, although in these cases we have not yet identified the phosphorylation sites. For PKG a site outside the N-terminus may be a possibility, as the closely related serotonin transporter undergoes PKG-dependent phosphorylation at a canonical PKG site in IL2 that is conserved in DAT (43). Finally, CaMKII has been invoked to phosphorylate DAT based on loss of CaMKII-dependence of AMPH-induced DA efflux after mutagenesis of N-terminal serines (15). Although regulation of DAT phosphorylation in response to modulation of CaMK has not been demonstrated, the robust phosphorylation of NDAT and DAT N-terminal peptide by CaMKII (15) supports this possibility.

Of the kinases we characterized for phosphoamino acid usage, the only ones that phosphorylated NDAT on Thr were the proline-directed kinases ERK1/2, p38, and JNK. These kinases require a proline immediately following the phosphoacceptor site, and catalyzed robust phosphorylation of Thr53 present within a proline-directed kinase motif close to the intracellular end of TM1. We verified the presence of pThr on the N-terminal tail of neuronal DAT and identified Thr53 as a phosphorylation site in heterologously expressed DAT. Because proline-directed motifs are not recognized by non-proline directed kinases these findings demonstrate that DAT is a direct *in vivo* substrate for ERK or other proline-directed kinases. We have not yet attempted to modulate phosphorylation of this site by activators or inhibitors of any of these kinases, so the identities of the enzymes that regulate this site remain to be determined. However, the potential for ERK to catalyze the Thr phosphorylation of DAT *in vivo* is supported by the suppression of DAT phosphorylation by the MEK inhibitor U0126 (32).

Several of kinases that we tested (PKCβI, PKCβII, PKCγ, and Akt) showed considerably lower activity against NDAT compared to ERK1 or PKCα. This suggests a lower probability for these kinases to act on DAT, although we cannot exclude the possibility that *in vivo* interactions with these kinases could be promoted by adaptor proteins or other conditions not present *in vitro*. As some of these kinases (PKCβII and Akt) participate in DAT regulatory mechanisms

(14,21), our findings are more consistent with effects of these pathways being mediated indirectly rather than through direct phosphorylation of DAT. The only kinase we tested that showed no detectable reaction with NDAT was GSK3β. However, GSK3β often requires a priming phosphorylation event on its substrates by a distinct kinase at a separate phosphoacceptor site (44), thus we do not know if our result for NDAT represents a true negative for GSK3β phosphorylation or a manifestation of a requirement for priming.

Of the kinases we tested, the highest stoichiometry of NDAT phosphorylation was catalyzed by ERK1/2, p38, and JNK, which also induced a conformational change that altered the peptide electrophoretic mobility. This confomational change is likely to be caused by cis-isomerization of the pThr-Pro bond, which is characteristic of proline-directed phosphorylation and well established to induce significant alterations in protein secondary structure (45). Whether phosphorylation at this site *in vivo* could be related to the multiple DAT bands commonly seen in western blots (37,46) or to previously noted upward shifts of DAT that accompany metabolic phosphorylation (13) is not known. However, the induction of such a conformational change by phosphorylation of Thr53 could significantly impact the properties of this domain.

Our finding that Thr53 is phosphorylated *in vivo* provides the first localization of pThr on DAT and the first evidence that phosphorylation occurs in the membrane proximal region of the N-terminal tail. Phosphorylation of this residue is not required for down-regulation mediated by ERK inhibition or PMA, and future work will be required to determine the function of this site. At present little is known about the structures or functions of the DAT cytosolic domains or how they might be affected by phosphorylation. Our current understanding of DAT structure is based on homology to the bacterial leucine transporter (LeuT), which does not possess the extensive cytoplasmic domains found in DAT (47), and provides little guidance regarding this issue. However, the proximity of phosphorylation to the intracellular end of TM1 suggests the potential to impact functions associated with this domain, including binding and permeation of substrates, binding of cocaine and other transport blockers, and ionic interactions between Arg60 and other intracellular gate residues (42,48-50). Proline-rich regions such as that surrounding Thr53 can also serve as binding sites for Src homology 3 domain proteins (51), which function to regulate protein-protein interactions. One possibility for function is interaction with DAT binding partners such as syntaxin (52), which could affect ion flow or efflux. The structural changes induced by PKC-dependent phosphorylation of the distal serine cluster and how these impact DAT functions are also unknown.

Very little is known about the role of dephosphorylation in DAT regulation. We previously found in rat striatal tissue that OA treatment down-regulates DA transport activity and leads to strong elevations in DAT phosphorylation indicative of significant tonic dephosphorylation (13,38). In the present study we found that NDATs phosphorylated by PKCα were extensively dephosphorylated by PP1, which parallels our previous findings of robust PP1-induced *in vivo* and *in vitro* dephosphorylation of PKC- and OA-stimulated phosphorylation sites on rDAT (38), and provides further evidence supporting the role of PP1 as the major DAT phosphatase. We also found for the first time that PP2B (calcineurin), caused a partial level of NDAT and rDAT dephosphorylation. The basis for the differential levels of NDAT and rDAT dephosphorylation by PP1 and PP2B is not known, although potential reasons include enzyme affinity for the peptide, phosphorylation site accessibility, and activity against different subsets of residues. Further work will be required to determine if DAT is dephosphorylated *in vivo* by PP2B, but if this occurs it would indicate the potential for a previously unknown mode of regulation of DAT phosphorylation levels by Ca^{+2}-calmodulin dependent mechanisms. Our finding that PP2A does not detectably dephosphorylate PKCα-phosphorylated NDAT or PMA-phosphorylated rDAT is consistent with our previous *in vitro* results and supports the lack of major PP2A effects on metabolic phosphorylation (38). However, further work is necessary to examine the role of PP2A, as the *in vitro* PP2A studies were performed with purified catalytic

subunit that lacks the scaffolding and regulatory subunits that may be necessary for driving enzyme-substrate interactions.

In contrast to our findings of significant *in vitro* dephosphorylation of PKC-catalyzed phosphorylation sites, none of the tested phosphatases were able to dephosphorylate ERK-phosphorylated NDATs. This may indicate that pThr53 requires a phosphatase different from those tested or that the altered conformation induced by Thr53 phosphorylation generates a peptide structure resistant to dephosphorylation. For many proteins including tau, Cdc25 and myc, ERK-catalyzed phosphorylation is removed primarily by PP2A, but this occurs only after the cis pSer/pThr-Pro conformation induced by phosphorylation is converted to the trans form by peptidyl–prolyl cis/trans isomerase (45,53). This could explain the phosphatase resistance of NDAT, because the cis-trans isomerization necessary to allow PP2A to dephosphorylate the peptide could not occur *in vitro*. Evidence that PP2A binds to DAT (54) suggests a role for this enzyme in DAT function. Our findings that DAT phosphorylation is only slightly increased by PP2A specific inhibitors (38), in conjunction with lack of PP2A effects on PKC-catalyzed sites could be consistent with a role for this enzyme at Thr53 or other site(s) distinct from those in the PKCα phosphorylated domain.

The results presented in this study demonstrate the ability of the recombinant DAT N-terminal domain to directly interact with several protein kinases and phosphatases, and for phosphorylation to occur at distinct sites. This is consistent with the regulation of DAT *in vivo* phosphorylation levels by multiple kinases (PKC, PKA, PKG, and ERK) and phosphatases (PP1 and PP2A) occurring by direct action of these enzymes. Phosphorylation of DAT by multiple kinases at distinct and/or overlapping sites could serve as a mechanism for integration of information from multiple pathways, or could provide a mechanism for different pathways to regulate distinct transporter functions. Because increasing evidence indicates that DAT regulation occurs by a combination of direct transporter phosphorylation and phosphorylation of interacting proteins (15,18,30,55), determining the details of these events is crucial for elucidating the mechanisms by which incoming physiological signals impact DA clearance in normal and disease states.

Acknowledgements

This work was supported by grants R01 DA13147 to R.A.V. from the National Institute on Drug Abuse, ND EPSCoR IIG to R.A.V. and J.D.Foster, ND EPSCoR Doctoral Dissertation Fellowship to B.K.G., P20 RR016741 to the University of North Dakota from the INBRE program of the National Center for Research Resources, and ND EPSCoR through NSF EPS-0447679.

ABBREVIATIONS

DAT, dopamine transporter
DA, dopamine
AMPH, amphetamine
METH, methamphetamine
PKC, protein kinase C
PKA, cAMP dependent protein kinase
PKG, cGMP dependent protein kinase
CAMKII, calcium-calmodulin protein kinase II
ERK, extracellular signal regulated kinase
PMA, phorbol 12-myristate, 13-acetate
OA, okadaic acid
PP1, protein phosphatase 1
PP2A, protein phosphatase 2A
PP2B, protein phosphatase 2B

pSer, phosphoserine
pThr, phosphothreonine
NDAT, N-terminal domain DAT recombinant protein
CDAT, C-terminal DAT recombinant protein

REFERENCES

1. Giros B, Jaber M, Jones SR, Wightman RM, Caron MG. Hyperlocomotion and indifference to cocaine and amphetamine in mice lacking the dopamine transporter. Nature 1996;379:606–612. [PubMed: 8628395]
2. Kuhar MJ, Ritz MC, Boja JW. The dopamine hypothesis of the reinforcing properties of cocaine. Trends Neurosci 1991;14:299–302. [PubMed: 1719677]
3. Eshleman AJ, Henningsen RA, Neve KA, Janowsky A. Release of dopamine via the human transporter. Mol Pharmacol 1994;45:312–316. [PubMed: 7906856]
4. Sulzer D, Chen TK, Lau YY, Kristensen H, Rayport S, Ewing A. Amphetamine redistributes dopamine from synaptic vesicles to the cytosol and promotes reverse transport. J Neurosci 1995;15:4102–4108. [PubMed: 7751968]
5. Weinberger DR, Egan MF, Bertolino A, Callicott JH, Mattay VS, Lipska BK, Berman KF, Goldberg TE. Prefrontal neurons and the genetics of schizophrenia. Biol Psychiatry 2001;50:825–844. [PubMed: 11743939]
6. Tintner R, Jankovic J. Treatment options for Parkinson's disease. Curr Opin Neurol 2002;15:467–476. [PubMed: 12151845]
7. Sawa A, Snyder SH. Schizophrenia: diverse approaches to a complex disease. Science 2002;296:692–695. [PubMed: 11976442]
8. Olanow CW. The role of dopamine agonists in the treatment of early Parkinson's disease. Neurology 2002;58:S33–S41. [PubMed: 11909983]
9. Mazei-Robison MS, Bowton E, Holy M, Schmudermaier M, Freissmuth M, Sitte HH, Galli A, Blakely RD. Anomalous dopamine release associated with a human dopamine transporter coding variant. J Neurosci 2008;28:7040–7046. [PubMed: 18614672]
10. Zahniser NR, Doolen S. Chronic and acute regulation of Na+/Cl− -dependent neurotransmitter transporters: drugs, substrates, presynaptic receptors, and signaling systems. Pharmacol Ther 2001;92:21–55. [PubMed: 11750035]
11. Melikian HE. Neurotransmitter transporter trafficking: endocytosis, recycling, and regulation. Pharmacol Ther 2004;104:17–27. [PubMed: 15500906]
12. Vaughan RA. Phosphorylation and regulation of psychostimulant sensitive neurotransmitter transporters. J Pharmacol Exp Ther 2004;310:1–7. [PubMed: 15064332]
13. Vaughan RA, Huff RA, Uhl GR, Kuhar MJ. Protein kinase C-mediated phosphorylation and functional regulation of dopamine transporters in striatal synaptosomes. J Biol Chem 1997;272:15541–15546. [PubMed: 9182590]
14. Garcia BG, Wei Y, Moron JA, Lin RZ, Javitch JA, Galli A. Akt is essential for insulin modulation of amphetamine-induced human dopamine transporter cell-surface redistribution. Mol Pharmacol 2005;68:102–109. [PubMed: 15795321]
15. Fog JU, Khoshbouei H, Holy M, Owens WA, Vaegter CB, Sen N, Nikandrova Y, Bowton E, McMahon DG, Colbran RJ, Daws LC, Sitte HH, Javitch JA, Galli A, Gether U. Calmodulin kinase II interacts with the dopamine transporter C terminus to regulate amphetamine-induced reverse transport. Neuron 2006;51:417–429. [PubMed: 16908408]
16. Moron JA, Zakharova I, Ferrer JV, Merrill GA, Hope B, Lafer EM, Lin ZC, Wang JB, Javitch JA, Galli A, Shippenberg TS. Mitogen activated protein kinase regulates dopamine transporter surface expression and dopamine transport capacity. J Neurosci 2003;23:8480–8488. [PubMed: 13679416]
17. Gulley JM, Doolen S, Zahniser NR. Brief, repeated exposure to substrates down-regulates dopamine transporter function in Xenopus oocytes in vitro and rat dorsal striatum in vivo. J Neurochem 2002;83:400–411. [PubMed: 12423250]

18. Cervinski MA, Foster JD, Vaughan RA. Psychoactive substrates stimulate dopamine transporter phosphorylation and down-regulation by cocaine-sensitive and protein kinase C-dependent mechanisms. J Biol Chem 2005;280:40442–40449. [PubMed: 16204245]
19. Gorentla BK, Vaughan RA. Differential effects of dopamine and psychoactive drugs on dopamine transporter phosphorylation and regulation. Neuropharmacology 2005;49:759–768. [PubMed: 16181646]
20. Kahlig KM, Javitch JA, Galli A. Amphetamine regulation of dopamine transport. Combined measurements of transporter currents and transporter imaging support the endocytosis of an active carrier. J Biol Chem 2004;279:8966–8975. [PubMed: 14699142]
21. Johnson LA, Guptaroy B, Lund D, Shamban S, Gnegy ME. Regulation of amphetamine-stimulated dopamine efflux by protein kinase C beta. J Biol Chem 2005;280:10914–10919. [PubMed: 15647254]
22. Saunders C, Ferrer JV, Shi L, Chen J, Merrill G, Lamb ME, Leeb-Lundberg LM, Carvelli L, Javitch JA, Galli A. Amphetamine-induced loss of human dopamine transporter activity: an internalization-dependent and cocaine-sensitive mechanism. Proc Natl Acad Sci U S A 2000;97:6850–6855. [PubMed: 10823899]
23. Loder MK, Melikian HE. The dopamine transporter constitutively internalizes and recycles in a protein kinase C-regulated manner in stably transfected PC12 cell lines. J Biol Chem 2003;278:22168–22174. [PubMed: 12682063]
24. Melikian HE, Buckley KM. Membrane trafficking regulates the activity of the human dopamine transporter. J Neurosci 1999;19:7699–7710. [PubMed: 10479674]
25. Foster JD, Adkins SD, Lever JR, Vaughan RA. Phorbol ester induced trafficking-independent regulation and enhanced phosphorylation of the dopamine transporter associated with membrane rafts and cholesterol. J Neurochem 2008;105:1683–1699. [PubMed: 18248623]
26. Johnson LA, Furman CA, Zhang M, Guptaroy B, Gnegy ME. Rapid delivery of the dopamine transporter to the plasmalemmal membrane upon amphetamine stimulation. Neuropharmacology 2005;49:750–758. [PubMed: 16212991]
27. Miranda M, Wu CC, Sorkina T, Korstjens DR, Sorkin A. Enhanced ubiquitylation and accelerated degradation of the dopamine transporter mediated by protein kinase C. J Biol Chem 2005;280:35617–35624. [PubMed: 16109712]
28. Daniels GM, Amara SG. Regulated trafficking of the human dopamine transporter. Clathrin- mediated internalization and lysosomal degradation in response to phorbol esters. J Biol Chem 1999;274:35794–35801. [PubMed: 10585462]
29. Goodwin JS, Larson GA, Swant J, Sen N, Javitch JA, Zahniser NR, De Felice LJ, Khoshbouei H. Amphetamine and methamphetamine differentially affect dopamine transporters in vitro and in vivo. J Biol Chem. 2008
30. Granas C, Ferrer J, Loland CJ, Javitch JA, Gether U. N-terminal truncation of the dopamine transporter abolishes phorbol ester- and substance P receptor-stimulated phosphorylation without impairing transporter internalization. J Biol Chem 2003;278:4990–5000. [PubMed: 12464618]
31. Huff RA, Vaughan RA, Kuhar MJ, Uhl GR. Phorbol esters increase dopamine transporter phosphorylation and decrease transport Vmax. J Neurochem 1997;68:225–232. [PubMed: 8978729]
32. Lin Z, Zhang PW, Zhu X, Melgari JM, Huff R, Spieldoch RL, Uhl GR. Phosphatidylinositol 3-kinase, protein kinase C, and MEK1/2 kinase regulation of dopamine transporters (DAT) require N-terminal DAT phosphoacceptor sites. J Biol Chem 2003;278:20162–20170. [PubMed: 12660249]
33. Gnegy ME. Ca2+/calmodulin signaling in NMDA-induced synaptic plasticity. Crit Rev Neurobiol 2000;14:91–129. [PubMed: 11513244]
34. Foster JD, Pananusorn B, Vaughan RA. Dopamine transporters are phosphorylated on N-terminal serines in rat striatum. J Biol Chem 2002;277:25178–25186. [PubMed: 11994276]
35. Foster, JD.; Blakely, RD.; Vaughan, RA. Abstract Viewer/Itinerary Planner. Society for Neuroscience Program No. 167.12; Washington, DC: 2003. Mutational analysis of potential phosphorylation sites in the N-terminal tail of the rat dopamine transporter..
36. Chang MY, Lee SH, Kim JH, Lee KH, Kim YS, Son H, Lee YS. Protein kinase C-mediated functional regulation of dopamine transporter is not achieved by direct phosphorylation of the dopamine transporter protein. J Neurochem 2001;77:754–761. [PubMed: 11331404]

37. Vaughan RA, Gaffaney JD, Lever JR, Reith ME, Dutta AK. Dual incorporation of photoaffinity ligands on dopamine transporters implicates proximity of labeled domains. Mol Pharmacol 2001;59:1157–1164. [PubMed: 11306699]
38. Foster JD, Pananusorn B, Cervinski MA, Holden HE, Vaughan RA. Dopamine transporters are dephosphorylated in striatal homogenates and in vitro by protein phosphatase 1. Brain Res Mol Brain Res 2003;110:100–108. [PubMed: 12573538]
39. Boyle WJ, van der Geer P, Hunter T. Phosphopeptide mapping and phosphoamino acid analysis by two- dimensional separation on thin-layer cellulose plates. Methods Enzymol 1991;201:110–149. [PubMed: 1943760]
40. Moritz, AE.; Gorentla, BK.; Vaughan, RA. Abstract Viewer/Itinerary Planner. Society for Neuroscience Program No. 249.21; Washington, DC: 2007. The N-terminal tail of the dopamine transporter is phosphorylated at multiple sites in vitro..
41. Clark Lewis I, Sanghera JS, Pelech SL. Definition of a consensus sequence for peptide substrate recognition by p44mpk, the meiosis activated myelin basic protein kinase. J Biol Chem 1991;266:15180–15184. [PubMed: 1907971]
42. Beuming T, Shi L, Javitch JA, Weinstein H. A comprehensive structure based alignment of prokaryotic and eukaryotic neurotransmitter/Na+ symporters (NSS) aids in the use of the LeuT structure to probe NSS structure and function. Mol Pharmacol 2006;70:1630–1642. [PubMed: 16880288]
43. Ramamoorthy S, Samuvel DJ, Buck ER, Rudnick G, Jayanthi LD. Phosphorylation of threonine residue 276 is required for acute regulation of serotonin transporter by cyclic GMP. J Biol Chem 2007;282:11639–11647. [PubMed: 17310063]
44. Frame S, Cohen P. GSK3 takes centre stage more than 20 years after its discovery. Biochem J 2001;359:1–16. [PubMed: 11563964]
45. Zhou XZ, Kops O, Werner A, Lu PJ, Shen M, Stoller G, Kullertz G, Stark M, Fischer G, Lu KP. Pin1-dependent prolyl isomerization regulates dephosphorylation of Cdc25C and tau proteins. Mol Cell 2000;6:873–883. [PubMed: 11090625]
46. Li LB, Chen N, Ramamoorthy S, Chi L, Cui XN, Wang LC, Reith ME. The role of N-glycosylation in function and surface trafficking of the human dopamine transporter. J Biol Chem 2004;279:21012–21020. [PubMed: 15024013]
47. Yamashita A, Singh SK, Kawate T, Jin Y, Gouaux E. Crystal structure of a bacterial homologue of Na+/Cl−-dependent neurotransmitter transporters. Nature 2005;437:215–223. [PubMed: 16041361]
48. Kniazeff J, Shi L, Loland CJ, Javitch JA, Weinstein H, Gether U. An intracellular interaction network regulates conformational transitions in the dopamine transporter. J Biol Chem 2008;283:17691–17701. [PubMed: 18426798]
49. Beuming T, Kniazeff J, Bergmann ML, Shi L, Gracia L, Raniszewska K, Newman AH, Javitch JA, Weinstein H, Gether U, Loland CJ. The binding sites for cocaine and dopamine in the dopamine transporter overlap. Nat Neurosci 2008;11:780–789. [PubMed: 18568020]
50. Indarte M, Madura JD, Surratt CK. Dopamine transporter comparative molecular modeling and binding site prediction using the LeuT(Aa) leucine transporter as a template. Proteins 2007;70:1033–1046. [PubMed: 17847094]
51. Sparks AB, Rider JE, Hoffman NG, Fowlkes DM, Quillam LA, Kay BK. Distinct ligand preferences of Src homology 3 domains from Src, Yes, Abl, Cortactin, p53bp2, PLCgamma, Crk, and Grb2. Proc Natl Acad Sci U S A 1996;93:1540–1544. [PubMed: 8643668]
52. Carvelli L, Blakely RD, DeFelice LJ. Dopamine transporter/syntaxin 1A interactions regulate transporter channel activity and dopaminergic synaptic transmission. Proc Natl Acad Sci U S A 2008;105:14192–14197. [PubMed: 18768815]
53. Pastorino L, Sun A, Lu PJ, Zhou XZ, Balastik M, Finn G, Wulf G, Lim J, Li SH, Li X, Xia W, Nicholson LK, Lu KP. The prolyl isomerase Pin1 regulates amyloid precursor protein processing and amyloid-beta production. Nature 2006;440:528–534. [PubMed: 16554819]
54. Bauman AL, Apparsundaram S, Ramamoorthy S, Wadzinski BE, Vaughan RA, Blakely RD. Cocaine and antidepressant-sensitive biogenic amine transporters exist in regulated complexes with protein phosphatase 2A. J Neurosci 2000;20:7571–7578. [PubMed: 11027216]

55. Mortensen OV, Larsen MB, Prasad BM, Amara SG. Genetic Complementation Screen Identifies a Mitogen-activated Protein Kinase Phosphatase, MKP3, as a Regulator of Dopamine Transporter Trafficking. Mol Biol Cell 2008;19:2818–2829. [PubMed: 18434601]

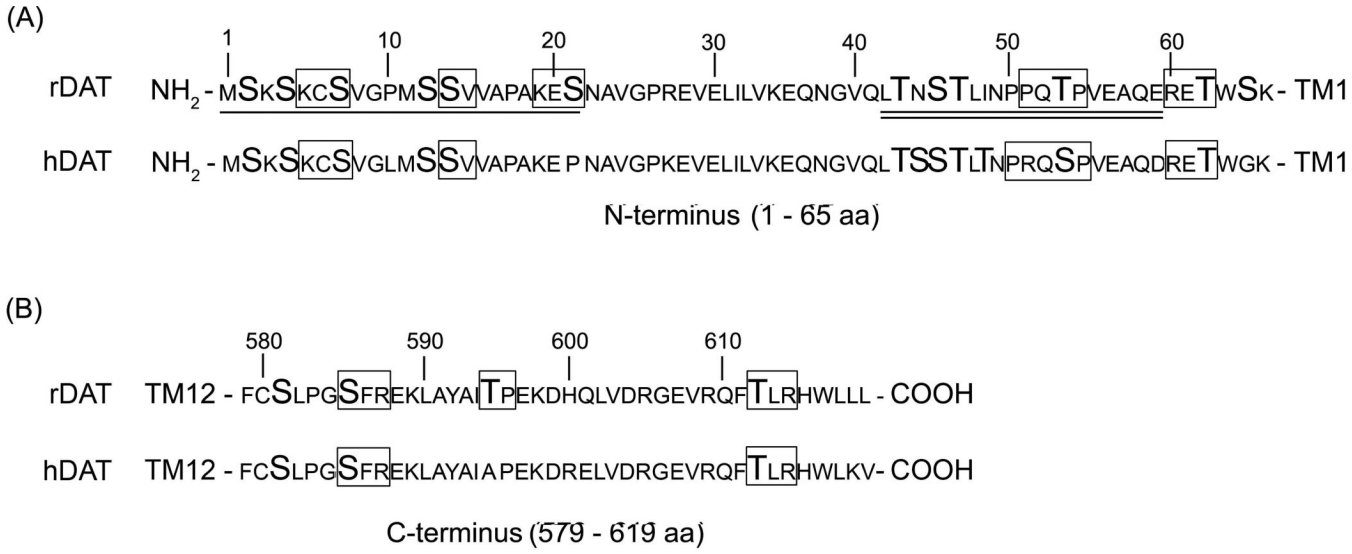

FIGURE 1.

DAT N- and C-terminal domains. Amino acid sequences of rat and human DAT N-termini (A) and C-termini (B). Serines and threonines are highlighted in large font, and consensus motifs for PKC, PKA, CaMK, and proline-directed kinases are enclosed by boxes. The N-terminal serine cluster of rDAT containing known *in vivo* phosphorylation sites is indicated with the single underline, and the epitope for Ab16 is shown with the double underline.

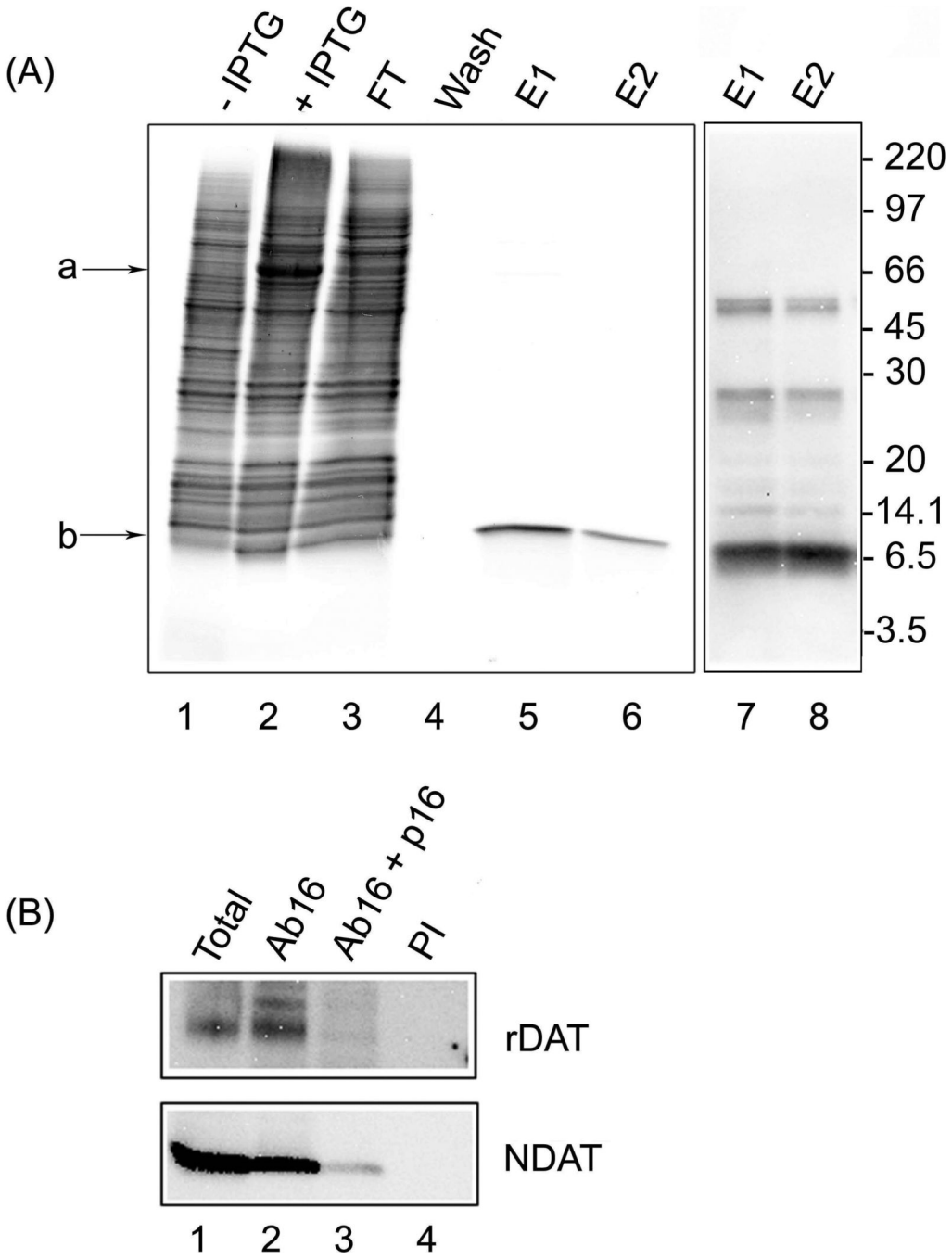

FIGURE 2.

Generation and characterization of NDAT. (A) Soluble lysates were prepared from *E. coli* cells transfected with NDAT-pTYB2 vector and treated with or without IPTG. Lysate from IPTG induced cells was affinity purified on chitin-Sepharose, and subjected to SDS-PAGE and staining with Coomassie blue (Lanes 1−6) or immunoblotting with mAb 16 (lanes 7 and 8). Lane 1, non-induced cells; lane 2, IPTG-induced cells; lane 3 column flow through; lane 4, final wash fraction; lanes 5 and 6, sequential elution fractions; lanes 7 and 8, elution fractions immunoblotted with mAb16. *Arrow a*, NDAT-CBD fusion protein. *Arrow b*, NDAT. (B). rDAT (upper panel) or NDAT (lower panel) were immunoprecipitated with Ab16 and analyzed by immunoblotting with mAb 16. Lane 1, input samples; lanes 2 and 3, samples precipitated

without (lane 2) or with (lane 3) peptide 16 preabsorption; lane 4, sample precipitated with preimmune (PI) serum. Molecular mass standards are shown in kDa.

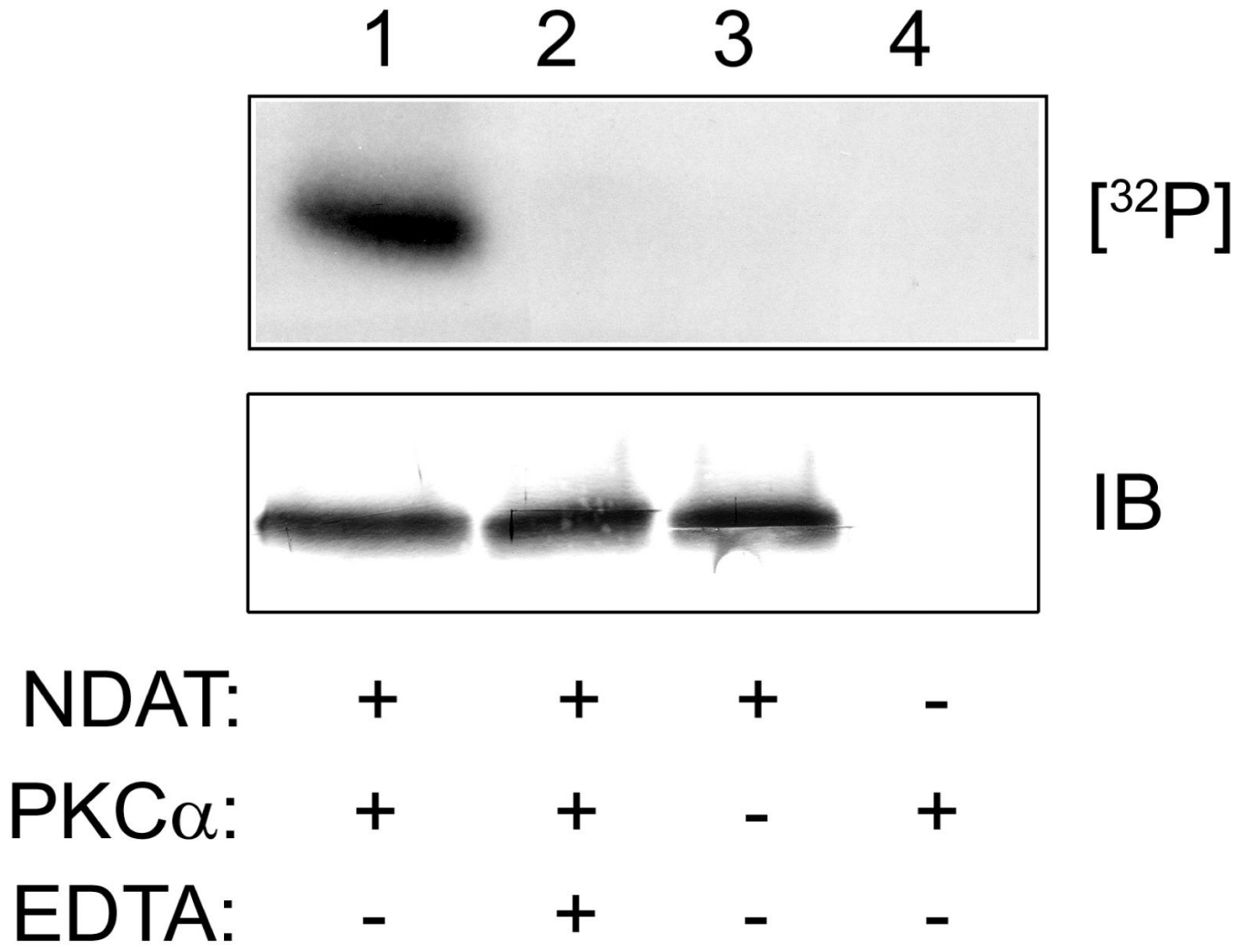

FIGURE 3.

In vitro phosphorylation of NDAT. NDAT was incubated with PKCα in a reaction mixture containing [γ-^{32}P]ATP and the indicated components. Lane 1, control reaction mixture; lane 2, reaction contained 100 mM EDTA; lane 3, reaction contained no PKCα, lane 4, reaction contained no NDAT. Samples were immunoprecipitated with Ab16 and analyzed by SDS-PAGE/autoradiography (upper panel) or immunoblotting (IB) (lower panel).

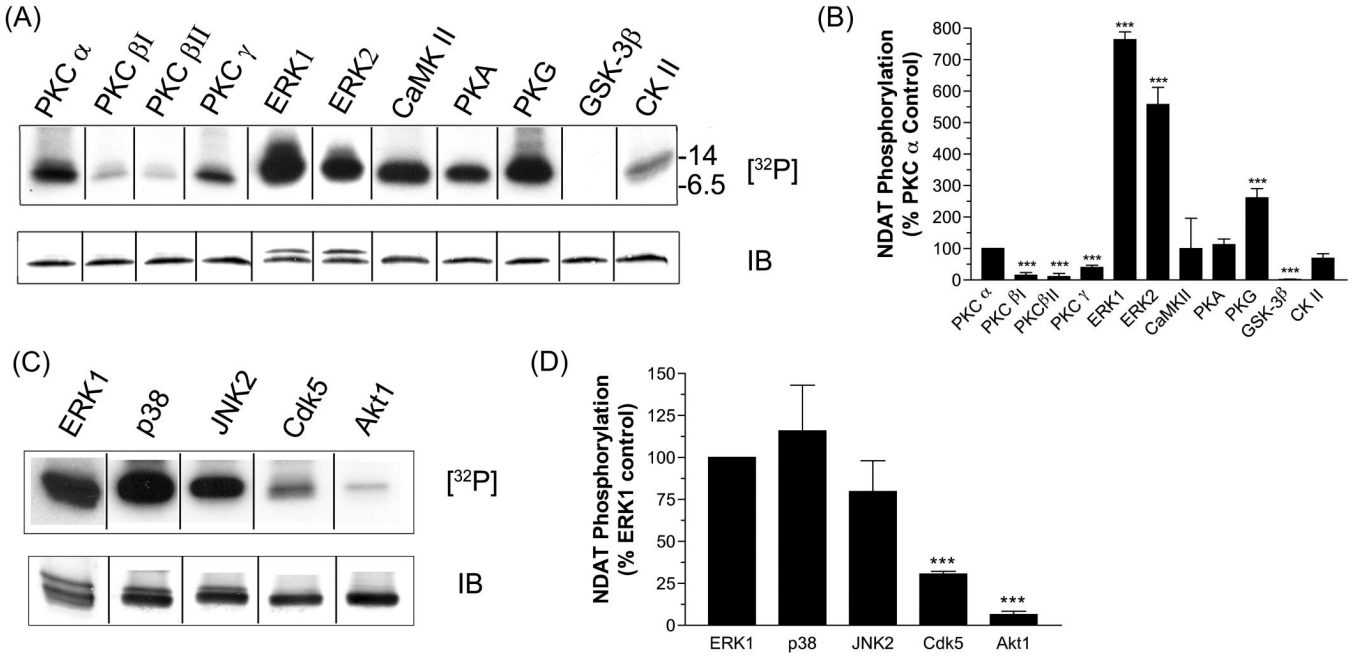

FIGURE 4.

Multiple kinases phosphorylate NDAT. Equal amounts of NDAT were subjected to *in vitro* phosphorylation with the indicated protein kinases followed by immunoprecipitation with Ab16 and SDS-PAGE/autoradiography (upper panels) or immunoblotting (IB) (lower panels). Panels A and C represent separate experiments with the immunoblot and autoradiograph obtained from aliquots of the same samples electrophoresed on separate gels in panel A, and the autoradiograph obtained from the immunoblot in panel C. Panels B and D show quantification of phosphorylation levels (means ± S.E. of two independent experiments) relative to PKCα (B) or ERK1 (D). *** $p < 0.001$ relative to indicated control.

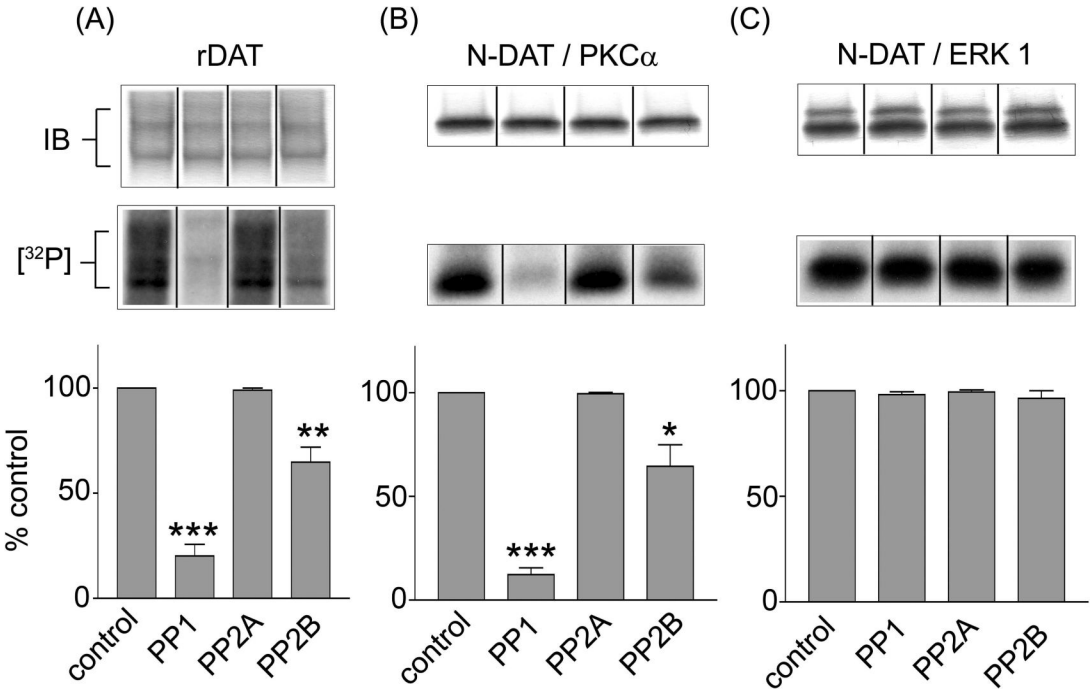

FIGURE 5.

In vitro dephosphorylation of NDAT. Metabolically phosphorylated rat striatal DAT (A) or NDAT phosphorylated *in vitro* by PKCα (B) or ERK1 (C) were immunoprecipitated and immune complexes incubated with PP1, PP2A or PP2B followed by immunoblotting (upper panel) or SDS-PAGE/autoradiography (middle panel). Gel lanes correspond to treatments indicated directly below on histogram. Lower panel: Quantification of NDAT or rDAT phosphorylation levels relative to control (means ± S.E. of three independent experiments). *p < 0.05 relative to control; **p < 0.01 relative to control; ***p < 0.001 relative to control, by ANOVA.

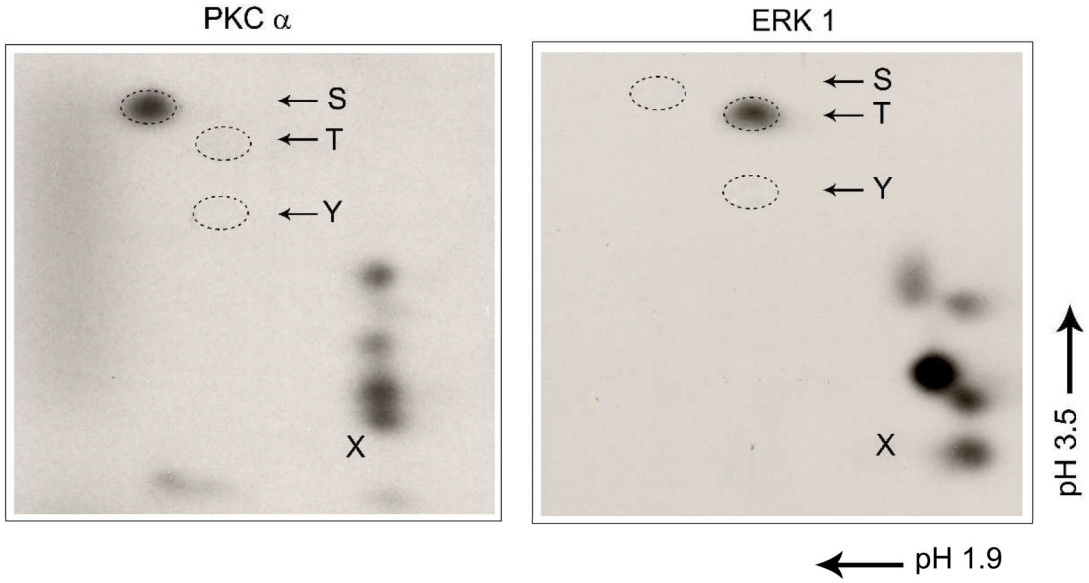

FIGURE 6.

Phosphoamino acid analysis of NDAT. NDATs phosphorylated by PKCα or ERK1 were gel purified and subjected to acid hydrolysis and 2D TLC in the presence of phosphoamino acid standards (dotted circles) followed by autoradiography. X, sample origin; S, pSer; T, pThr; Y, pTyr.

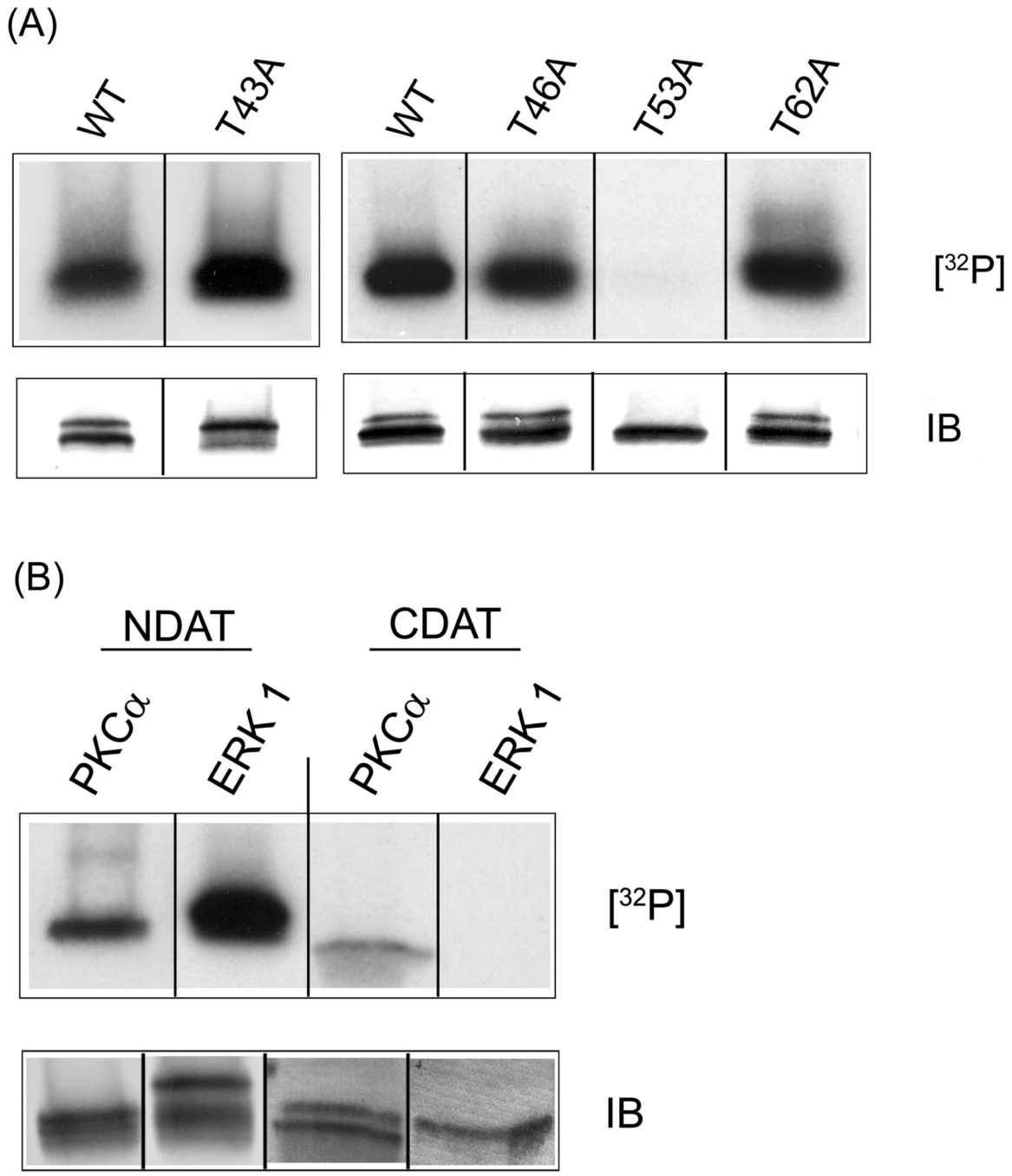

FIGURE 7.

ERK1 phosphorylates NDAT on Thr53. (A). Equal amounts of WT or T→A mutant NDATs were incubated with ERK1 under phosphorylation conditions followed by immunoprecipitation and autoradiography (upper panel) or immunoblotting (lower panel). Samples in left and right panels were analyzed in separate experiments. (B) Equal amounts (1.5 μg) of NDAT or CDAT were subjected to phosphorylation conditions with PKCα or ERK1 followed by immunoprecipitation, SDS-PAGE and autoradiography (upper panel) or immunoblotting (lower panel).

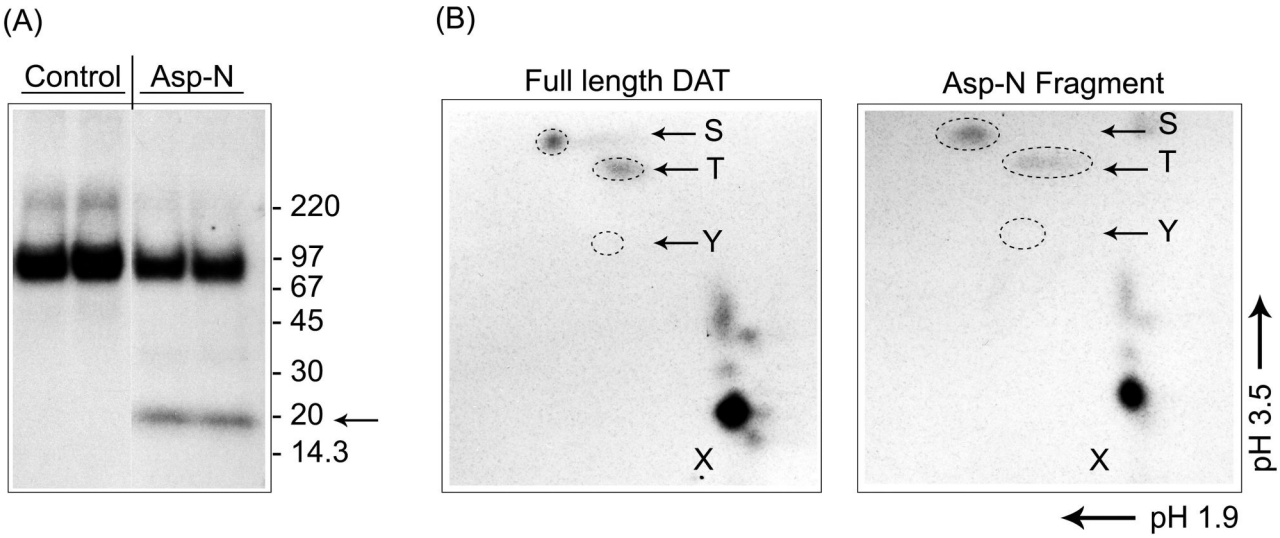

FIGURE 8.

Identification of phosphothreonine in the rDAT N-terminal tail. (A) Membranes from ^{32}P metabolically labeled rat striatal slices were treated with endoproteinase Asp-N followed by immunoprecipitation with Ab16 and SDS-PAGE/autoradiography. Full length DAT and Asp-N fragments (*arrow*) were excised from the gel and processed for phosphoamino acid analysis. (B) TLC plates containing samples from the full-length DAT and Asp-N fragments were subjected to autoradiography, and phosphoamino acid standards were visualized with ninhydrin (dotted circles). X, origin; S, pSer; T, pThr; Y, pTyr.

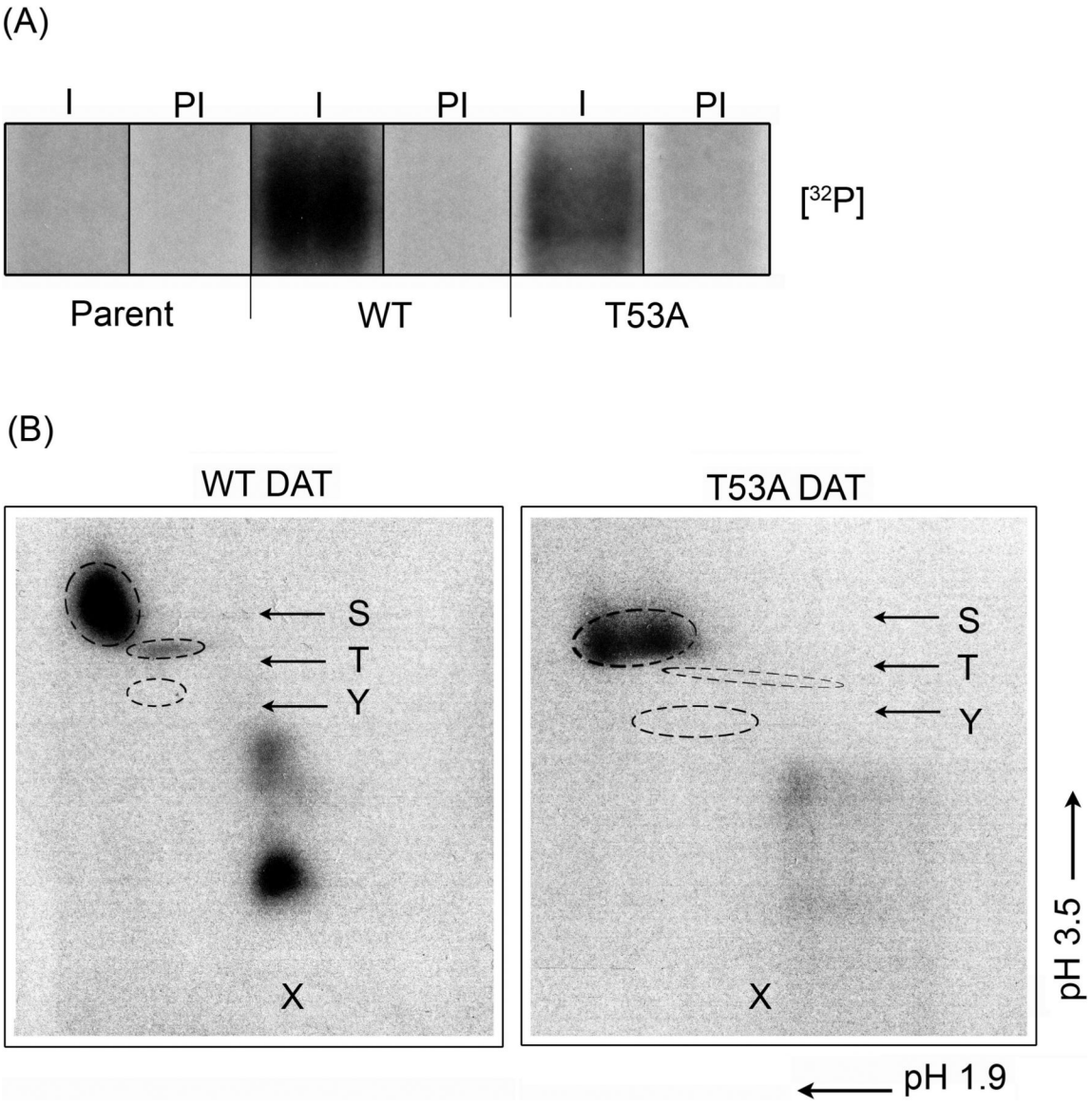

Figure 9.

Phosphothreonine is not present in T53A rDAT. LLCPK$_1$ cells expressing WT or T53A rDAT were labeled with $^{32}PO_4$ and treated with 1 μM PMA for 30 min. Samples from parent LLCPK$_1$ cells were treated and processed exactly in parallel for analysis of signal specificity. (A). Lysates were precipitated with immune (I) or preimmune (PI) serum and analyzed by SDS-PAGE/autoradiography. (B). WT and T53A DATs were extracted and equal counts subjected to phosphoamino acid analysis. Phosphoamaino acid standards were visualized with ninhydrin (dotted circles). X, origin; S, pSer; T, pThr; Y, pTyr.